Subcontractor Report

Plasma-Assisted Coevaporation of S and Se for Wide Band Gap Chalcopyrite Photovoltaics

**Phase II Annual Report
December 2002–December 2003**

I. Repins
*ITN Energy Systems, Inc.
Littleton, Colorado*

C. Wolden
*Colorado School of Mines
Golden, Colorado*

NREL

National Renewable Energy Laboratory

Plasma-Assisted Coevaporation of S and Se for Wide Band Gap Chalcopyrite Photovoltaics

Phase II Annual Report
December 2002–December 2003

I. Repins
ITN Energy Systems, Inc.
Littleton, Colorado

C. Wolden
Colorado School of Mines
Golden, Colorado

NREL

National Renewable Energy Laboratory

NOTICE

Available electronically at http://www.osti.gov/bridge

Available for a processing fee to U.S. Department of Energy
and its contractors, in paper, from:

U.S. Department of Energy
Office of Scientific and Technical Information
P.O. Box 62
Oak Ridge, TN 37831-0062
phone: 865.576.8401
fax: 865.576.5728
email: reports@adonis.osti.gov

Available for sale to the public, in paper, from:
U.S. Department of Commerce
National Technical Information Service
5285 Port Royal Road
Springfield, VA 22161
phone: 800.553.6847
fax: 703.605.6900
email: orders@ntis.fedworld.gov
online ordering: http://www.ntis.gov/ordering.htm

TABLE OF CONTENTS

LIST OF FIGURES

1. Introduction, Goals, and Approach

In terms of small-area device efficiency and module stability, $CuIn_xGa_{1-x}Se_2$ (CIGS) devices provide a benchmark for thin film photovoltaics. Nonetheless, there is significant opportunity for improvement in manufacture of CIGS devices. First, high-quality CIGS deposition requires high substrate temperatures (>500°C), limiting the selection of substrate materials and increasing deposition cycle times due to heat-up and cool-down periods. Furthermore, current co-evaporation technology requires overpressure of chalcogens (Se_2 or S_2) during deposition, resulting in low material utilization and high equipment maintenance costs. Furthermore, the useful available energy bandgap expansion via alloying is limited to less than 1.3 eV.

In this work, ITN Energy Systems (ITN) and lower-tier subcontractor Colorado School of Mines (CSM) explore the replacement of the molecular chalcogen precursors during deposition (e.g. Se_2 or H_2Se) with more reactive chalcogen monomers or radicals (e.g. Se). Molecular species are converted to atomic species in a low-pressure inductively-coupled plasma (ICP). Tasks of the proposed program center on development and validation of monatomic chalcogen chemistry, tuning of low-pressure monomer chalcogen sources, and evaluation of plasma-assisted co-evaporation (PACE) for CIGS co-evaporation. Likely advantages of deposition by plasma-enhanced co-evaporation include:

- Providing potential for lower deposition temperature and/or for better film quality at higher deposition temperature.
- Providing potential for decreased deposition times.
- Providing high material utilization efficiency (~90%) that results in less deposition on other parts of the reactor leading to lower clean up and maintenance costs, as well as longer equipment lifetime. High material utilization efficiency also reduces the total operating pressure, which is beneficial for the design and control of metal co-evaporation. Advantages include minimal metal-vapor beam spread and lower source operating temperatures.
- Enabling deposition of wide bandgap copper indium gallium disulfur-selenide (CIGSS) films with controlled stoichiometry.

University researchers at CSM are developing and testing the fundamental chemistry and engineering principles. Industrial researchers at ITN are adapting PACE technology to CIGSS co-evaporation and validating PACE process for fabrication of thin film photovoltaics. In_2Se_3 films, which are used as precursor layers in high-efficiency CIGS depositions, were used this year as the first test case for the examining the advantages of PACE listed above. Gradually, the investigation is being extended to the complete high-efficiency three-stage co-evaporation process.

The energetics involved in $CuInSe_2$ and $CuInS_2$ formation are illustrated in Figure 1. This diagram shows the changes in Gibbs free energy for $CuInSe_2$ (left) and $CuInS_2$ (right) synthesis from various chalcogen sources.[1,2] The formation energy of copper and indium are zero, so the reactant energy simply reflects the chalcogen source. Sulfur and selenium both sublime as dimers that may readily oligomerize into ring structures of S_n or Se_n, where n varies from 2 < n < 8. However, the variation of n between 2 and 8 has relatively little effect on the reactant energy. For example, the energetics of a sublimated S source would be bound between the S_2 and S_8 values shown in the right half of Figure 1.

---

[1] 78th Edition of the CRC Handbook of Chemistry and Physics, 78th Ed, Editor D. R. Lide, (CRC Press, Boca Raton) 1997.

[2] H. Migge and J. Grzanna, "Thermochemistry in the system Cu-In-S at 723K," *J. Mater. Chem.*, **9** (1994.) pp. 125-128.
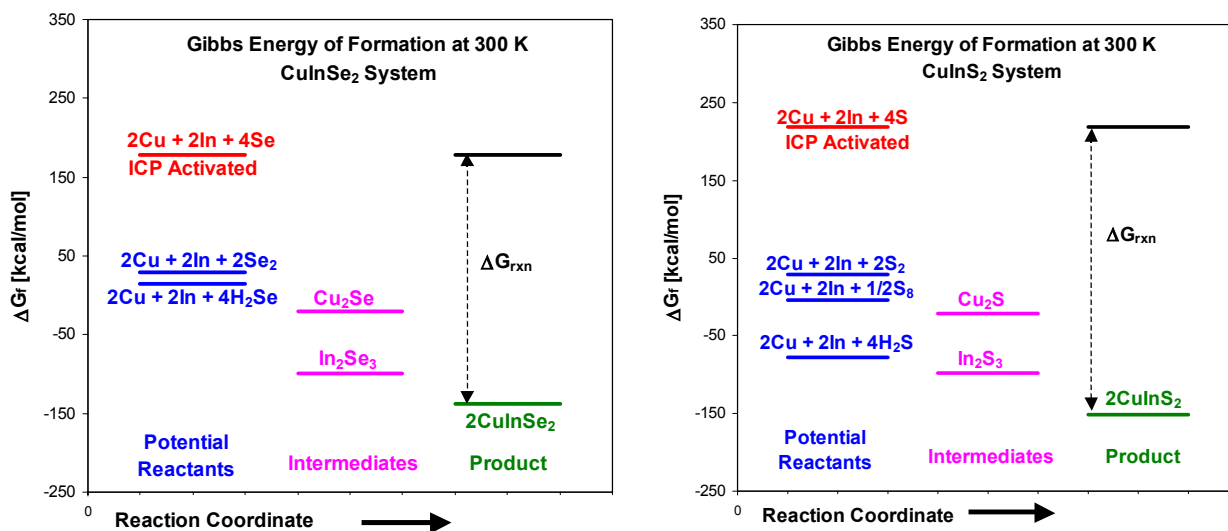
Figure 1: Thermodynamics of CuInSe₂ and CuInS₂ formation at 300 K using various chalcogen sources.

The details of the CIS reaction pathway are still somewhat of an open question. The formation of $CuInSe_2$ may occur directly, or it may proceed through the formation of the sulfide intermediates Cu_2Se and In_2Se_3. ***In either case significant activation barrier(s) must be present since the reaction does not proceed spontaneously at ambient conditions.*** The premise of this work is to overcome these barriers by activating the chalcogen source. This premise can be illustrated by considering, for example, the energy of S in its various states. At 300 K the free energy of sublimated S is near zero. The alternative hydrogen sulfide source is significantly more stable at this temperature. Our approach is to activate these chalcogen precursors using an inductively coupled plasma (ICP) source. In the plasma, high-energy electrons dissociate these feed gasses into atoms, excited metastables (S^*), and ions (S^+). Atomic sulfur provides a tremendous amount of energy, as was illustrated in Figure 1. The Gibbs heat of reaction using atomic sulfur would be very exothermic, -185 kcal/mol of $CuInS_2$. Metastable and ionic sulfur would provide even more energy to the system. The selenium system behaves very similarly, but the energy differences are slightly less dramatic. The dissociation of the selenium dimer requires ~88 kcal/mol versus ~95 kcal/mol for the sulfur dimer.[1] ICP devices have proven very efficient for dissociation of the dimers (H_2, O_2, Cl_2) used in chemical vapor deposition and etching processes.[3,4] The plasma kinetics of chalcogens have not been studied. However in the case of oxygen, a molecule that has nearly the same bond strength as S_2, nearly complete dissociation is achieved in these devices.[4]

During this phase, work has progressed in three main areas: investigating the effect of plasma activation on binary films, optimizing the ICP sources, and integrating the ICP sources into the full three-stage CIGS co-evaporation process. Highlights include room temperature formation of In_2Se_3 and Cu_2Se, and operation of the ICP sources at rates, pressures, and sizes consistent with three-stage co-evaporation. Work is described in further detail in the following sections.

---

[3] M. V. Malyshev and V.M. Donnelly, "Diagnostics of chlorine inductively coupled plasmas. Measurement of electron temperatures and electron energy distribution functions," *J. Appl. Phys.,* **87** (2000) pp. 1642-1648.

[4] E. Meeks, R.S. Larson, P. Ho, C. Apblett, S. M. Han, E. Edelberg, and E. S. Aydil, "Modeling of SiO_2 deposition in high density plasma reactors and comparisons of model predictions with experimental measurement," *J. Vac. Sci. Technol. A*, **16** (1998) pp. 544-563.

2. Effect of Plasma-Activation on Binary Films

The efficacy of plasma-activation for reducing required reaction temperature and increasing chalcogen utilization was examined during this phase. Plasma-activation was proven to be beneficial in reducing reaction temperatures for all binary precursors utilized in CIGSS formation: In_2Se_3, In_2S_3, Cu_xSe_y, and Cu_xS_y. A detailed study of improvements to materials utilization is also underway.

The effect of plasma-activation on binary films was examined during this phase primarily using the benchtop plasma source at CSM. The benchtop plasma source allows extensive quantification of sulfur/selenium flux and optimization ICP operation without use of complicated multiple-species rate monitors, or contamination of other equipment. The plasma is contained in a 1" diameter pyrex tube. Argon is supplied through a needle valve, while an on/off valve isolates the chalcogen effusion source. A butterfly valve on the exhaust line is used to control the pressure. The effusion source is maintained at the desired temperature through PID control. This benchtop unit is operated at the similar conditions as will be used for CIGS film depositions, except that the system is exhausted directly to a pump, instead of effusing into a high vacuum environment.

Plasma-activation was proven beneficial in reducing reaction temperature for all binary precursors utilized in CIGSS formation: In_2Se_3, In_2S_3, Cu_xSe_y, and Cu_xS_y. Without plasma activation or heating, In+Se and Cu+Se films are amorphous. For example, Figure 2 shows x-ray diffraction (XRD) patterns from evaporated Se co-delivered with sputtered In or Cu, with a 1.5:1 chalcogen to metals ratio. The films are largely amorphous. No peaks of magnitude comparable to the Mo peaks from the underlying back contact are apparent. Such spectra are consistent with those reported in the literature.[5]
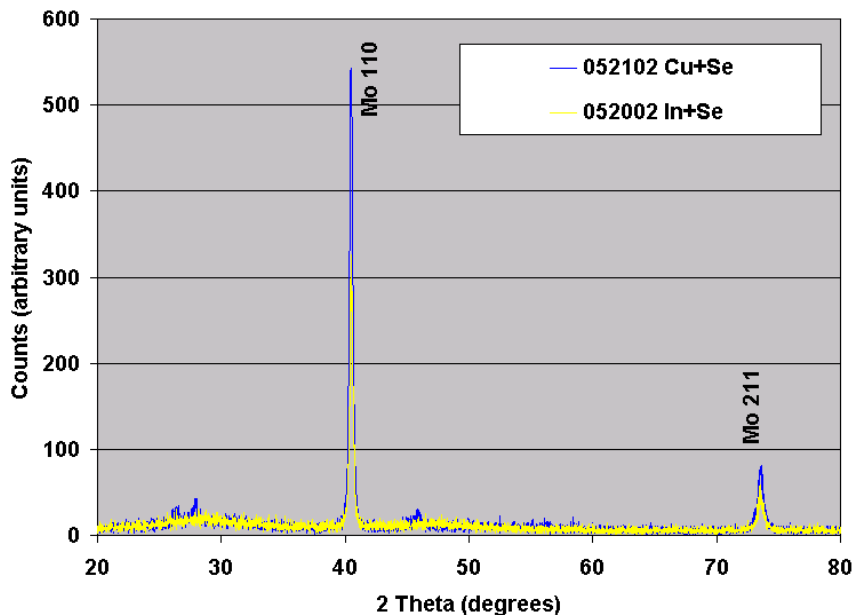
Figure 2: XRD patterns for Cu+Se and In+Se films co-delivered at room temperature.

[5] See, for example, M.E. Beck, A. Swartzlander-Guest, R. Matson, J. Keane, R. Noufi, "CuIn(Ga)Se2-Based Devices Via a Novel Absorber Formation Process", *Solar Energy Materials & Solar Cells*, **64**(2), pp. 135-165, (2000).

In contrast, under standard conditions (i.e. those typically used in the first stage of the three-stage recipe), all peaks in the XRD pattern of the precursor can be assigned to In_2Se_3. An example of a standard In_2Se_3 XRD pattern is shown in Figure 3. This film was made in ITN's bell jar, under standard three-stage co-evaporation conditions: 325 ^oC, Se and In co-delivered in a 5-to-1 ratio.
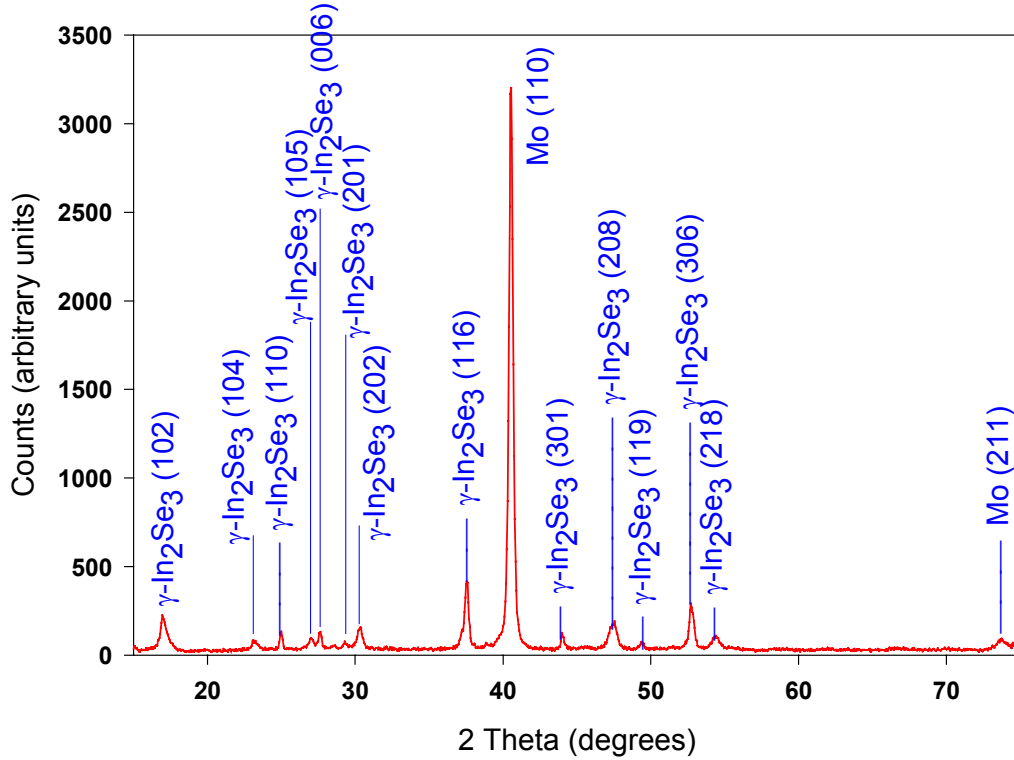
Figure 3: XRD pattern from standard co-evaporated In_2Se_3 film, with peak assignments.

Utilizing the PACE benchtop source at CSM, binary chalcogenides were formed at room temperature. In contrast with the amorphous, conventional films of Figure 2, those formed using plasma activation were highly crystalline chalcogenides. Figure 4a shows the XRD patterns generated before (pink) and after (blue) exposing In foil to plasma-activated Se at room temperature. A complete conversion of the In to In_xSe_y compounds occurs. Similar data is shown in Figure 4b for exposure of the In to S. Figure 4c shows the evolution of Cu to Cu_xSe_y with increased exposure times to plasma-activated Se. Figure 4d shows the complete conversion of Cu foil to Cu_xS_y after exposure to plasma-activated S. These data illustrate the efficacy of PACE for decreasing reaction temperatures of CIGS precursors, a second-year milestone.

The benchtop plasma-activation source has been modified to allow a novel and time-efficient method for further study of the temperature dependence of plasma-assisted reactions. A resistively-heated and PID-controlled substrate temperature stage was installed inside the benchtop plasma-activation source. Both the heating element and the thermocouple are sheathed and grounded, and temperature is controlled during plasma operation with no observable impact on the plasma itself. Temperatures up to 600 ^oC are easily obtained. For the next phase, the new capability also allows investigation of the selenization of Cu-In-Ga films, which has proven problematic at ambient temperature.

4
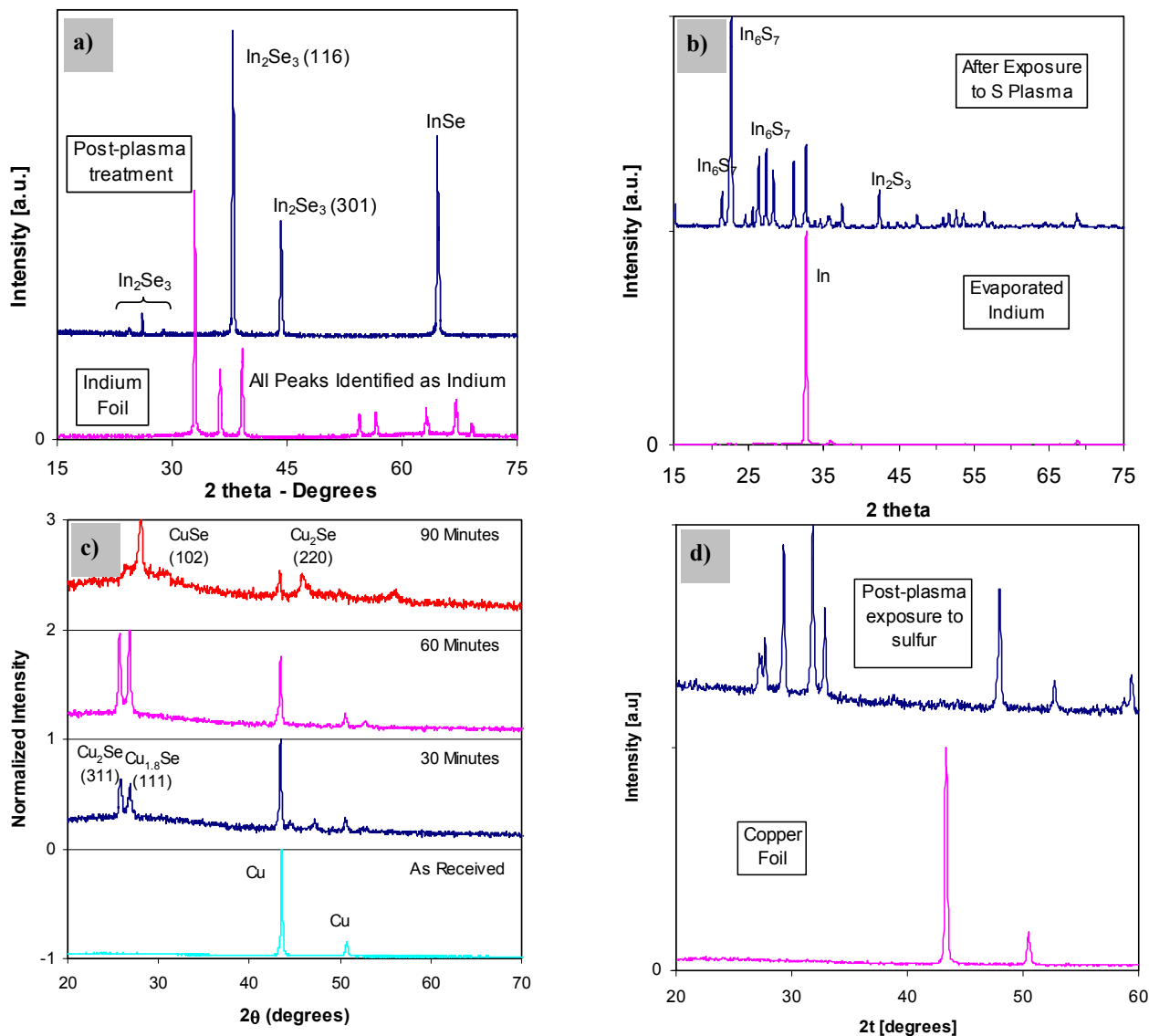
Figure 4: XRD patterns generated before and after exposing In to plasma-activated chalcogens at room temperature. a) shows exposure of In foil to plasma-activated Se, b) shows exposure of evaporated In to plasma-activated S, c) shows exposure of sputtered Cu to plasma-activated Se as a function of time S, d) shows exposure of sputtered Cu to plasma-activated S.

The efficacy of plasma-activation for increasing chalcogen utilization is currently under examination utilizing co-delivered In and Se fluxes in the CSM PACE chamber. The PACE chamber allows the study of plasma-activated binary film formation and source uniformity without the stringent requirements on temperature and multi-source flux rate monitoring imposed by full CIGSS co-evaporation. The PACE chamber includes is a glass bell jar equipped with a quartz crystal microbalance (QCM), an evaporation source for metals, and the ICP enhanced Se source. The substrate is radiatively heated and maintained at the desired setpoint using PID control.

A chalcogen utilization study requires precise knowledge of the ratio of chalcogen to metals fluxes during co-deposition. Thus, careful calibration is being performed. It is necessary to account for variable film density when calibrating the QCM via profilometry measurements: A discrepancy between the apparent thicknesses of indium films evaporated at different substrate temperatures is observed. For the same nominal QCM deposition rate, films deposited on a heated substrate are significantly thicker as measured by profilometry. Data indicates that the difference is related to film density: i.e. the films on heated substrates are less dense, resulting in thicker films for the same mass deposition rate. Figure 5 compares atomic force microscopy (AFM) data from films deposited at 20 ºC and 200 ºC. The films deposited at 200 ºC have much larger grains, and the roughness is an order of magnitude larger. The films deposited at ambient temperature have much smaller grains and a smoother texture.

(a) T_s = 20 ºC
RMS Roughness = 30 nm

(b) T_s = 200 ºC
RMS Roughness = 285 nm
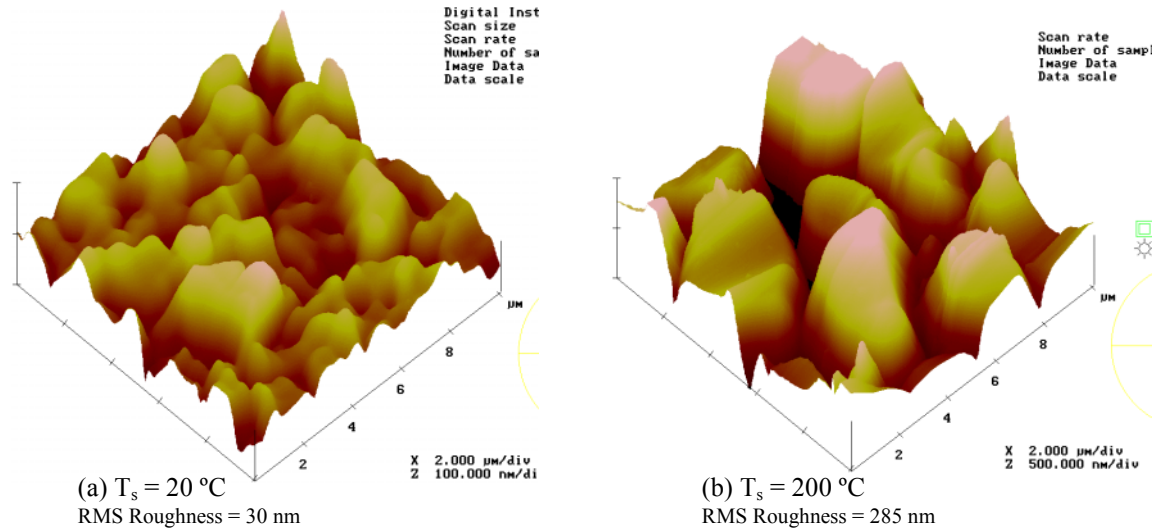
Figure 5: AFM images and root mean square (RMS) roughness values of films deposited at (a) room temperature and (b) 200 ºC. Note that the z-scale is 5X greater in (b).

The AFM images suggest that surface mobility engendered by the higher temperature leads to the coalescence of larger grains. As these larger grains are formed, they may lead to shadow effects at the microscale, causing to a columnar porous structure that has a lower density. Thus it is concluded that the QCM detector, which is always water-cooled, provides an accurate measure of the mass deposition rate, but not necessarily the linear deposition rate. The impact of this effect during co-evaporation will be studied as materials utilization experiments continue. Utilization of the chalcogen optical emission lines from the ICP device is also underway for a highly-accurate, non-contact chalcogen rate monitor.

3. Source Development

During this phase, the ICP sources were developed to a point allowing reliable operation under conditions similar to those in CIGS co-evaporation. The advances made during this phase include reliable delivery of Se into plasma reactor tube, acceptable rate control, improvements in source size, minimizing transmitted RF, demonstrating satisfactory base pressures with Ar flow to the PACE source, and examination of source uniformity. Figure 6 shows a PACE source operating in the glass bell jar at CSM. On the left is shown the entire bell jar, with a close up of reactor tube shown on the right.
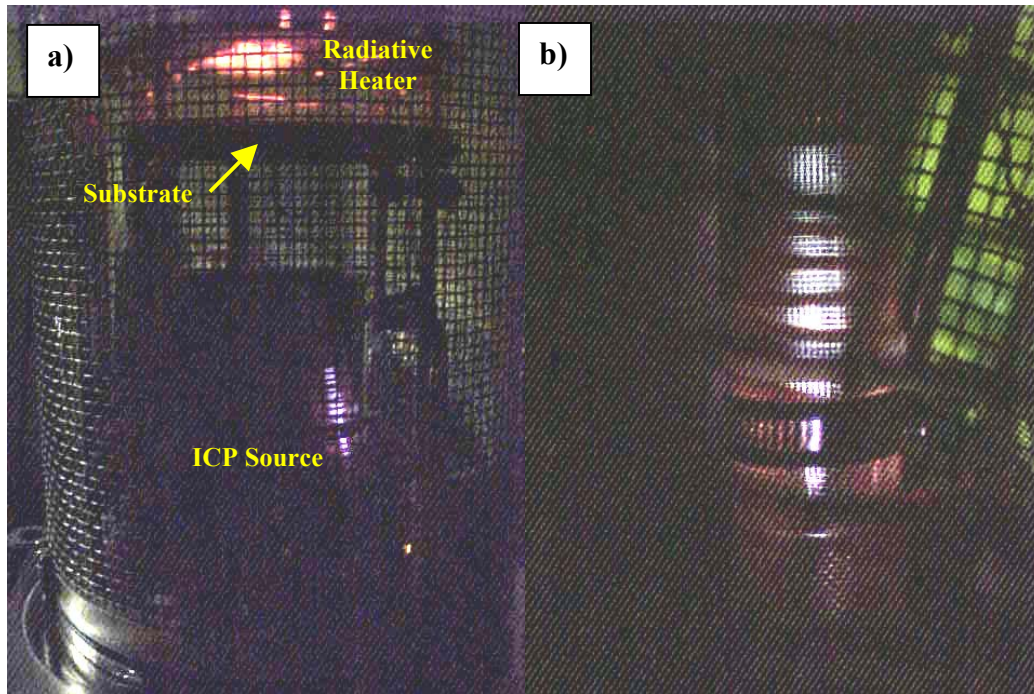
Figure 6: PACE source operating in glass bell jar at CSM. Photos show a) entire bell jar, and b) close up of reactor tube therein.

One of the major achievements in this phase is the development of reliable Se delivery into the plasma source. Chalcogen delivery in the co-evaporative environment was investigated using two approaches. These approaches are illustrated in Figure 7. In the first approach, chalcogen flux is controlled mainly by the effusion source temperature. Advantages of this first approach include large source capacity and capabilities for high Se pressures. In the second approach, chalcogen flux is controlled mainly by the hot carrier gas temperature. Advantages of the second approach include reduced thermal time constants and reduction of condensation between the Se source and the ICP device.
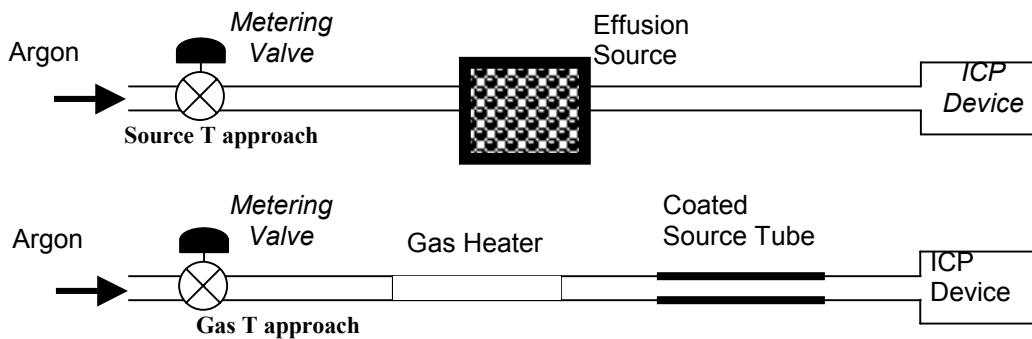
Figure 7: Schematic comparison of two approaches for chalcogen delivery.

Testing of the first approach was performed at ITN using both high- and low-current effusion sources. The high-current effusion source tested was a commercially-available Ta baffled box. Use of the Ta box is attractive as it is relatively low-cost, is conveniently re-loaded, and adequate Se control has been proven under other conditions: Similar sources are used in conjunction with a QCM in CIGS

co-evaporation. However, several problems were encountered with the Ta box source. First, the high-current feedthroughs to the box, in conjunction with the ICP quartz tube attached to the box, made the entire source difficult to fit into the bell jar. Second, the combination of Ar and Se pressure caused the lids used for Se loading to blow off the source. Finally, the brittleness of the Ta caused frequent source failures when adjustments to the source were made.

A tightly-sealed stainless steel source utilizing high voltage and low current heating rods was fabricated to circumvent the difficulties associated with the high-current effusion source. Use of molecular beam epitaxy and valved thermal cracker sources was also investigated but not pursued due to high cost. The low-current stainless steel effusion source was operated with acceptable control in conjunction with the quartz plasma tube and Ar gas. This control was achieved by minimizing source pot thermal mass, avoiding Se condensation via heating vapor tubing and the Ar gas prior to its entry to the source, and tuning proportional integral derivative (PID) control loops. Figure 8 shows Se rate as a function of time for the source, both with and without the quartz plasma tube in place. Rate was measured by a QCM placed 1" above the source opening. Se rate with the quartz tube in place is somewhat irregular compared to the rate without, but is still inside an acceptable envelope for CIGS co-evaporation. Source temperatures at the Se melt and at the source nozzle are also shown in Figure 8.

Figure 8: Se rate from PACE effusion source a) without and b) with quartz reactor tube. Effusion source temperature is also shown.

8

The second Se-delivery approach of Figure 7 (hot carrier gas) was examined at CSM. The combination of low Ar thermal mass, low Ar flow, and low ICP device operating pressure made Se vaporization difficult. Thus, the thermal effusion source approach was determined to be favorable.
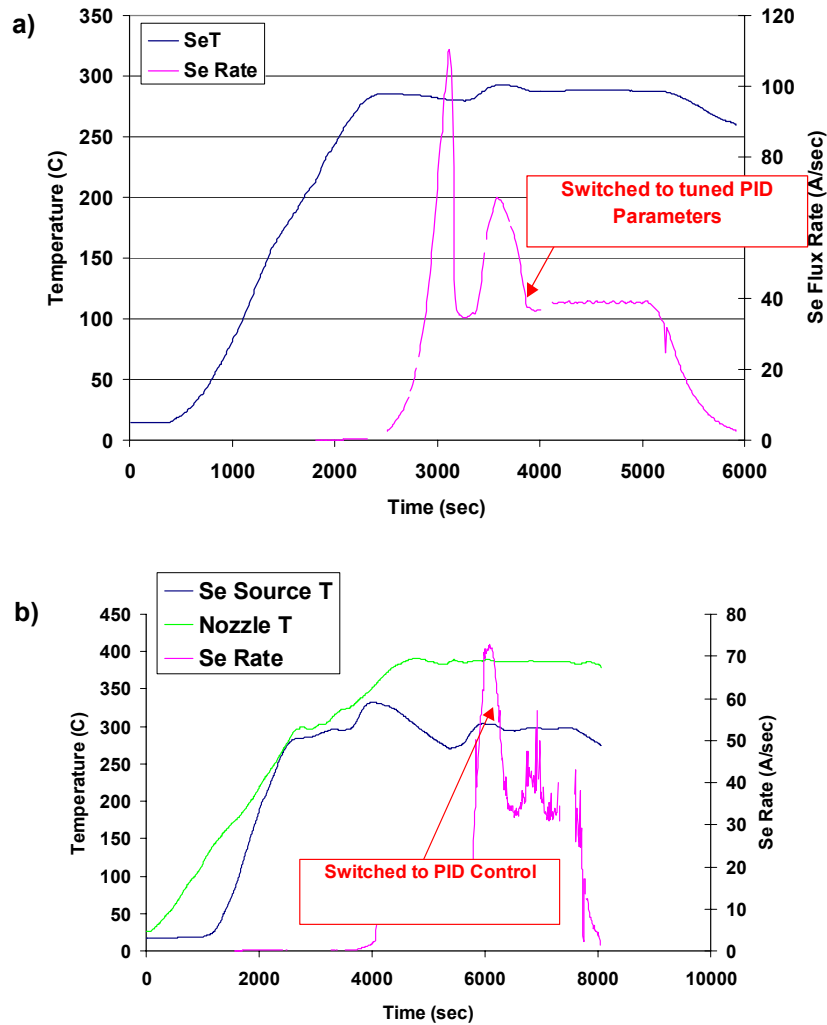
During this phase, RF transmission from the ICP sources was minimized to an extent that it does not interfere with other components. In the PACE chamber at CSM, stainless steel shielding was fabricated and installed to separate the indium evaporation source and the selenium ICP source. The shielding is well-grounded, acting as a Faraday cage to limit RF noise from the plasma. The arrangement allows stable operation of the ICP source without influencing the QCM, substrate heater, evaporation source, or instrumentation. It prevents indium deposition from occurring on the ICP source.

Satisfactory base pressures with Ar flow to the PACE source were also demonstrated. Figure 9 plots the relationship between the ICP pressure as measured by a convection gauge upstream of the actual device and the PACE chamber pressure as measured by a cold cathode gauge. Since the ICP gauge is upstream of the ICP device, the true pressure in the ICP device is estimated to be ~25% of the measured pressure due to friction drop and expansion in the line. Figure 9 shows that the two pressure regimes are effectively decoupled. The chamber pressure is approximately 4 orders of magnitude less than the ICP source. Best ICP device operations occurs around 100 mtorr, which means chamber pressure will be around 10^{-5} torr for depositions.

It should be noted that the relationship between ICP and chamber pressure is very sensitive to the size of the reactor tube orifice. Furthermore, the Ar pressure required for a stable plasma depends on the reactor tube geometry. Thus, as the reactor tubes are custom-made glassware, small variations from one reactor tube to the next may cause a significant modification to the relationship graphed in Figure 9.
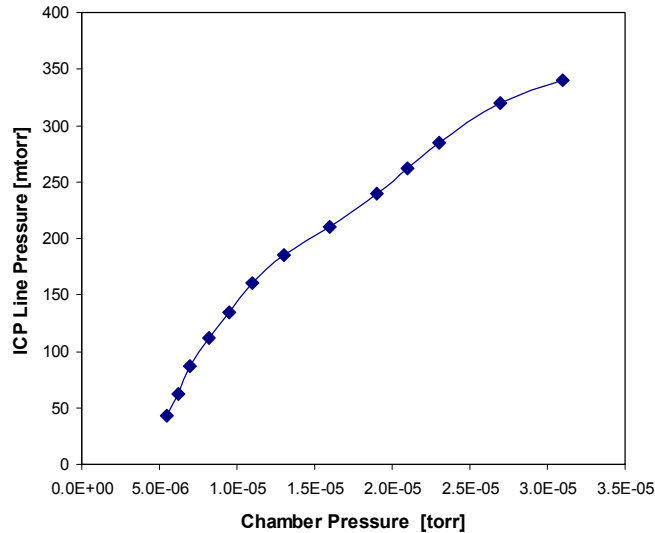
Figure 9: Relationship between ICP line pressure and PACE chamber pressure.

Improvements were also made to the PACE source length. The first source designed, shown on the left side of Figure 10 was more than 14" in length. This original dimension makes incorporation into CIGS co-evaporation impractical: It is longer than the distance from the baseplate to the substrate in ITN's bell jar. Several steps were taken to decrease source length. First, a gooseneck was built into the source interconnects. However, decreased rate controllability, most likely due to limited flow of Se vapor through the gooseneck, was observed. Next, all unnecessary length was trimmed from each component. The resulting design, shown on the right side of Figure 10, is approximately 5.5" tall. In Figure 10, most of each reactor tube is covered by metal shielding. Thus, the inset shows a magnification of the reactor tube orifice to indicate where Se exits the source.
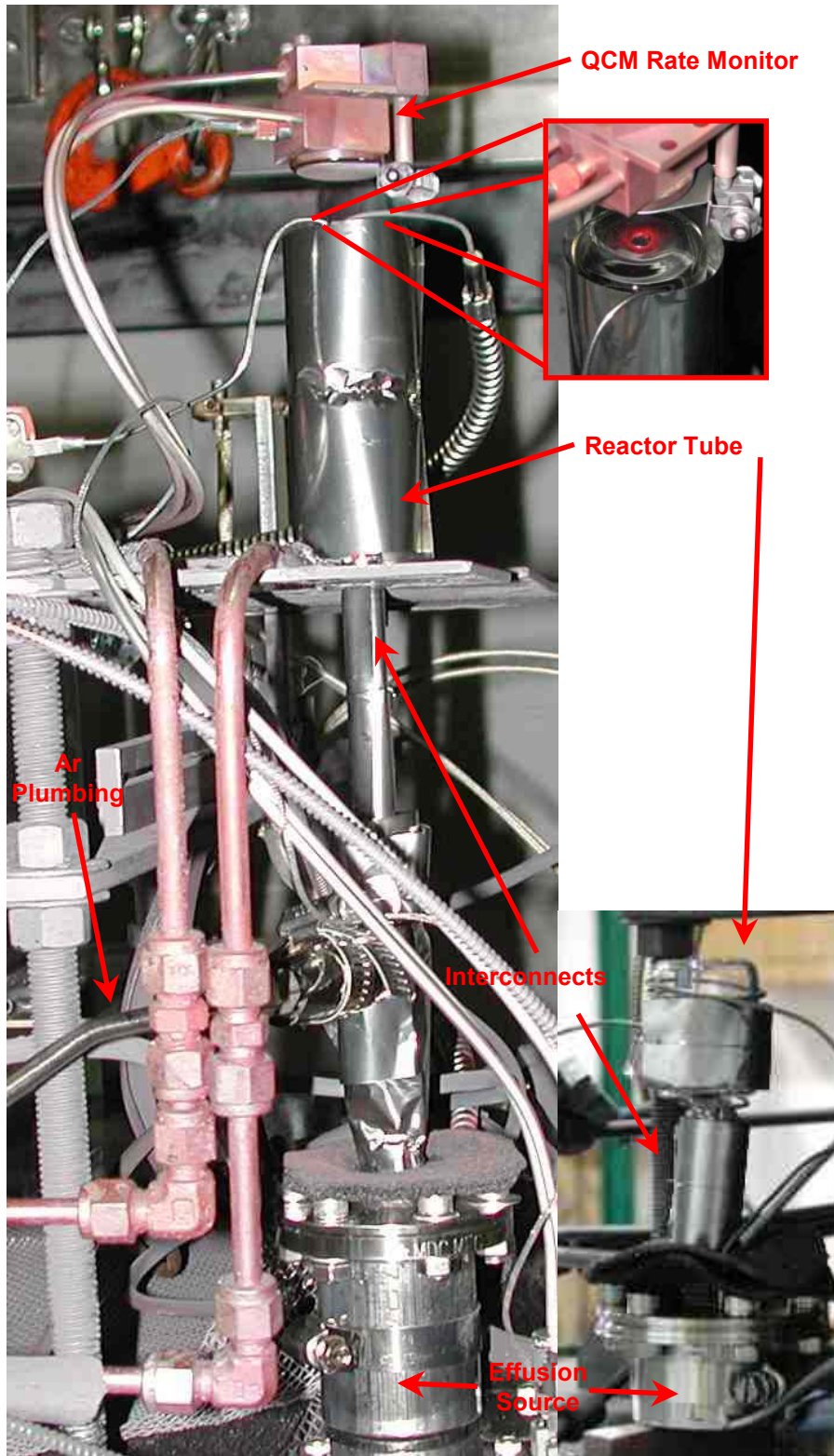
Figure 10: Photos of first (left) and more compact (right) source designs shown 50% of actual size. Inset is magnification of reactor tube orifice.

The spatial uniformity of Se flux from the compact PACE source was examined. A QCM was placed directly over the reactor tube aperture at 5.9" distance, and witness slides were arranged around the QCM. Profilometry was used to measure thickness at several points on the witness slides. Data are shown in Figure 11. The x axis in Figure 11 shows distance from the substrate center (QCM) to the measurement point, while the y axis shows Se thickness at that point. A least squares fit is shown in blue. The flux per solid angle fit is performed to $M\cos^n(\theta)$, where M and n are fit parameters, and θ is the azimuthal angle. The resulting n value is approximately 3, as has been reported elsewhere for effusion sources.[6,7] No measurements are available between 0 and 1" due to witness slide placement and film disadhesion. The film disadhesion is most likely due to the proximity of the witness slides to the heated reactor tube and the resulting thermal expansions. To form a more complete picture of source uniformity, work is ongoing to obtain thickness data at several radial distances smaller than 1", as well as to examine rate and controllability as a function of substrate distance from the aperture.
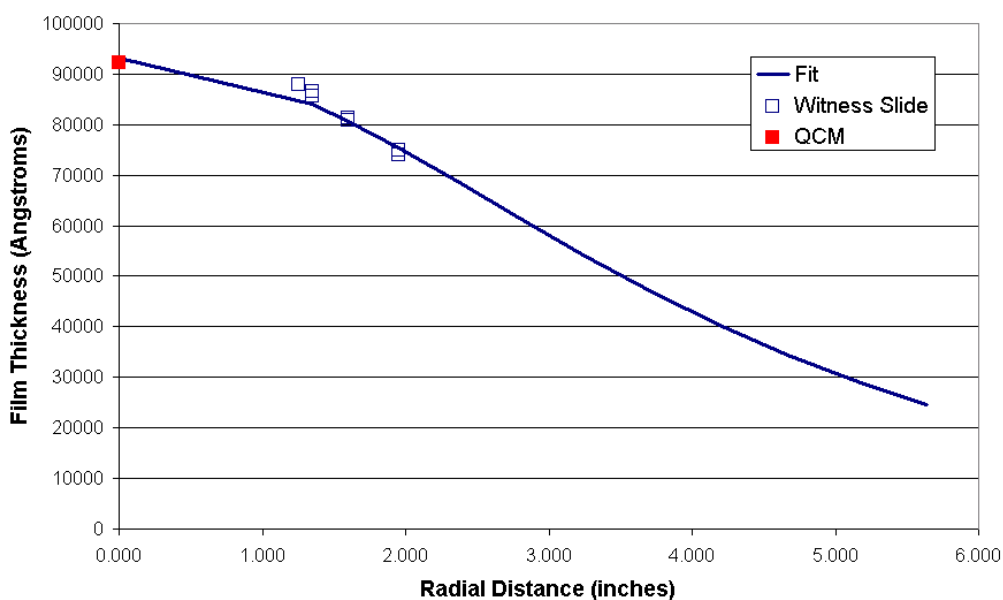
Figure 11: Se thickness as a function of distance from center of substrate.

The developments reported in this section comprise the specification of source geometry, control, reliability, and flux spatial uniformity that is milestone 2 for phase 2 in the statement of work.

4. Baseline CIGS Co-Evaporation Process

As described in the previous annual report, a baseline CIGS co-evaporation process was established in a bell jar at ITN. This standard process provides co-evaporated films to compare with the

---

[6] R.W. Birkmire, W.N. Shafarman, E. Eser, S.S. Hegedus, B.E. McCandless, R. Aparicio, K. Dobson, "Optimization of Processing and Modeling Issues for Thin Film Solar Cell Devices Including Concepts for the Development of Polycrystalline Multijunctions", *Annual Report to NREL under Subcontract ZAK-8-17619-33*, 2001, pp. 3-4.

[7] M.E. Beck, I.L. Repins, "Tolerance of Three-Stage CIGS Deposition to Variations Imposed by Roll-to-Roll Processing" *Annual Report to NREL Under Subcontract ZDJ-2-30630-14*, (2003), pg. 13 ff.

binary PACE films made at CSM, and serve in the upcoming phase as a testbed for integration of PACE into three-stage CIGS co-evaporation.

This year, several aspects of the baseline process were improved. Reproducibility was improved by insuring a consistent Cu-rich excursion of the film growth, using an infrared sensor to monitor the film emissivity change as it crosses in and out of the Cu-rich regime. This method is similar to those described elsewhere using a contact thermocouple to sense the temperature change resulting from the emissivity change.[8,9] Also, consistent incorporation of Ga was established via tuning source PID parameters and reliable calibration of the electron impact emission spectrometer (EIES) Ga reading. Overall, best efficiencies in the bell jar were improved from just over 10% last year to 12.5% this year. Figure 12 shows an example of a CIGS device from the bell jar, with all layers deposited at ITN. Device is 1 cm^2, with no anti-reflective coating. Quoted characterization is under AM1.5, total-area conditions.

The inset reads:

B030826-1
η = 12.5 %
Voc = 0.547 V

Jsc = 33.6 mA/cm^2
ff = 0.68
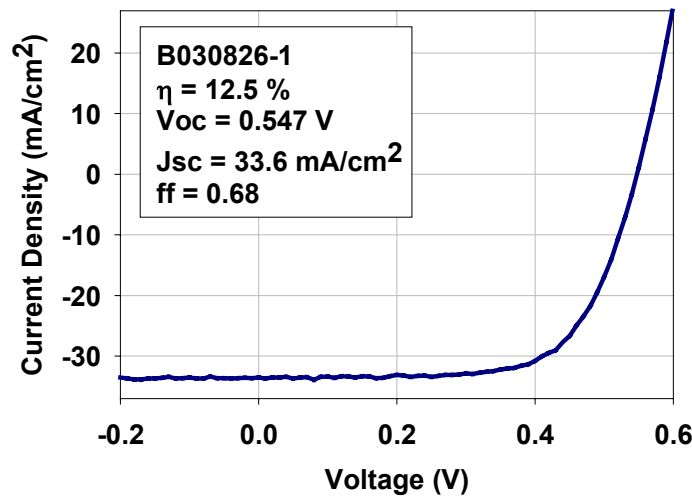
Figure 12: JV curve of small area device from bell jar. No AR coating was applied. Cell parameters shown in inset.

High efficiencies and low variability are important aspects of the baseline process. High efficiency is important to insure that conclusions drawn regarding PACE under this program are relevant to state-of-the-art CIGS devices made in other laboratories. Low variability is needed in order to unambiguously quantify the benefits of PACE on CIGS device quality in the next phase. Thus, minor adjustments to maximize baseline efficiency and reproducibility will continue under the next phase.

5. Integration of Plasma Sources into CIGS Co-Evaporation

Another area of progress this year is work toward the integration of plasma sources into full CIGS co-evaporation. (To date, the sources have been operated only in the fabrication of binary films, or in

---

[8] J. Kessler, J. Scholdstrom, L. Stolt, "Rapid Cu(In,Ga)Se$_2$ Growth Using "End Point Detection", *Proceedings of the 28th IEEE Photovoltaics Specialists Conference*, (2000), pp. 509-512.

[9] K. Ramanathan, M.A. Contreras, C.L. Perkins, S. Asher, F. S. Hasoon, J. Keane, D. Young, M. Romero, W. Metzger, R. Noufi, J. Ward, A. Duda, "Properties of 19.2% Efficiency CuInGaSe$_2$ Thin-film Solar Cells", *Progress in Photovoltaics: Research and Applications*, Vol. **11**, (2003), pp. 225-230.

diagnostic mode.) Incorporation of the plasma sources into three-stage CIGS co-evaporation is nontrivial, as the deposition environment exacts rigorous requirements on rate control, geometry, uniformity, resistance to heat and deposition product, and compatibility with the existing and complex sensors in the bell jar (e.g. EIES, QCM, IR). Plans to address these issues in the next phase were formulated this year. The issues, questions raised, related data, and plans are enumerated below.

1. **Geometry.** *Does the ICP source fit in the available space? If not, what modifications can be made to the source or the co-evaporation bell jar?*
   The recently-implemented compact PACE source (see Figure 10) will fit into the CIGS bell jar without interfering without other sources and sensors. Figure 13 shows the relevant dimensions in a cut-out photograph of ITN's CIGS bell jar. The substrate sits 11.5" above the baseplate, and the PACE source needs to remain outside a 6" radius from the baseplate center to avoid interfering with metals evaporation sources and rate sensors. This arrangement leaves about 13" between the substrate and the bottom of the PACE source. The recent 5.5" source fits well into this space, unlike the original 14" version.
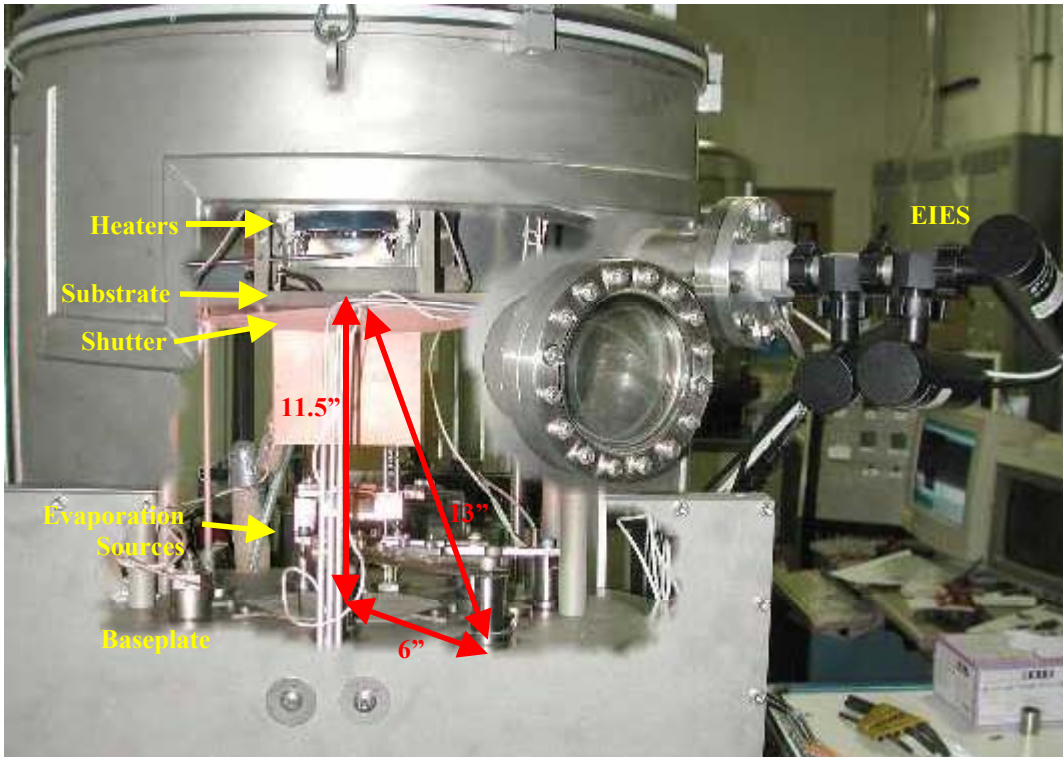
Figure 13: Photograph of CIGS bell jar with relevant dimensions for source geometry.

2. **Uniformity.** *One goal of PACE is increased chalcogen utilization. If this goal is achieved, the usual chalcogen overpressure will not be required and uniformity will be more important. What is the flux profile from the ICP sources as a function of geometry variables? Is uniformity sufficient?*
   Initial data and calculations indicate that uniformity from the present source design should be adequate. Data was presented earlier (Figure 11) suggesting that effusion from the PACE source follows the expected $\cos^3$ distribution. Measurements closer to the distribution center will be gathered during the next phase to verify this profile. Utilizing the $\cos^3$ distribution, calculated uniformity of the activated chalcogen over the 3" x 3" substrate is shown in Figure 14. Because of the competing effects of the $\cos^3$ profile, which decreases as one moves away from the point at which the nozzle is directed, and $1/r^2$ fall-off, which yields higher fluxes directly above the angled source, best uniformity should be achieved by pointing the source slightly beyond the substrate center. The calculations of Figure 14 indicate about 25% nonuniformity over the 3" x 3" substrate, sufficient to evaluate the efficacy of PACE in the bell jar and take

advantage of expected reductions in required Se overpressure. During the next phase, these uniformity estimations should be verified in-situ.

Figure 14: Calculated PACE uniformity over substrate, based on initial measurements.

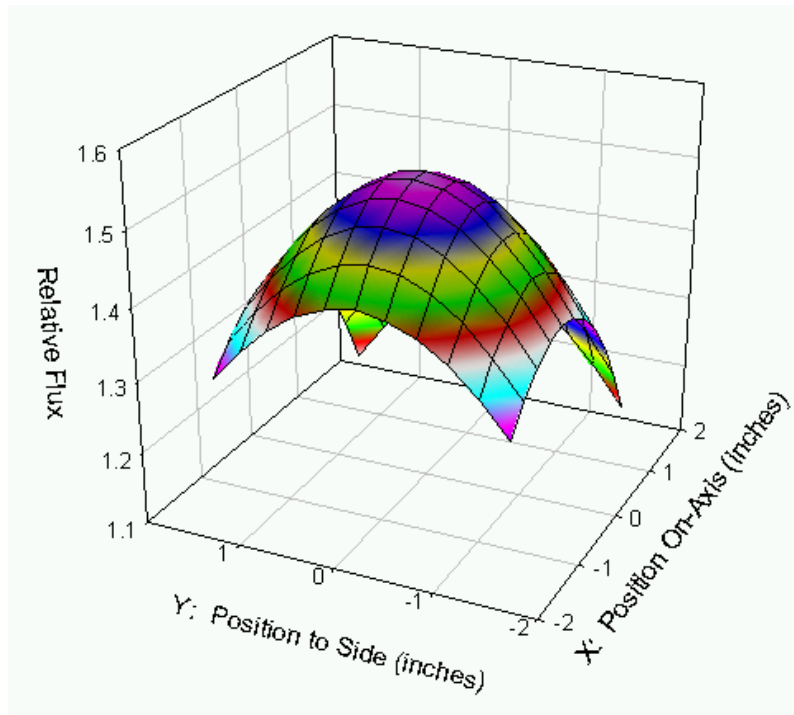**3. Rate.** *Can the sources deliver chalcogen at the necessary three-stage rates, for the appropriate geometry? Is the rate control responsive enough insure that the ICP rate profiles are comparable to those of the non-activated three-stage Se source?*

Initial data (see Figure 8) indicated that the PACE sources can be controlled well at rates consistent with the CIGS three-stage process. However, when source and substrate configuration is fully-specified, rate control should be re-examined. Relevant matters include evaluating rate control at several source-to-substrate distances, establishing a procedure allowing shorter warm-up times than that of Figure 8, and optimizing PID parameters with current and future in-situ geometry.

4. Equipment requirements. *How must the co-evaporation bell jar be modified to incorporate the ICP sources? Examples of items to consider are Ar gas flow, RF power and shielding, magnitude of the current to chalcogen source.*

It appears that necessary hardware can be added to the CIGS bell jar with only moderate disruption. Use of low-current, high-voltage Se effusion source provides flexibility in placement of the current feedthroughs relative to the PACE source. Effective solutions for grounding and shielding issues have been demonstrated in the CSM PACE chamber. Additional baseplate holes may be required for RF power feedthroughs. However, a method for machining these holes in place, without disassembling the chamber, using a drill with magnetic hold-down, has been identified. Ar plumbing, successfully utilized with the PACE source in its test environment, can be moved to the bell jar. This installation will be performed in the upcoming year.

5. Increased pressure and EIES noise. *The EIES rate monitor on the co-evaporation bell jar is sensitive to background pressure. How will the addition of small amounts of Ar from the ICP source affect the EIES readings? Do the EIES requirements place limits on the operating conditions of the ICP sources?*

Current data suggest that the PACE sources will exhibit only limited compatibility with the EIES rate monitor. The data shown earlier in Figure 10 predict a 10^{-5} Torr background pressure of Ar during PACE source operation. Such pressures will add significant background noise to the already weak EIES signal. The interference will be particularly severe for Ga, which is the weakest emitter of the three metals monitored by EIES. For illustration, Figure 15 shows apparent flux profiles from a CIGS deposition in which background pressure reached 8×10^{-6} Torr by the end of the second stage, due to an outgassing problem. Cu, In, and Ga rates graphed are those indicated by the EIES. Se rate is that indicated by the QCM. During the second stage (where the Cu rate is nonzero) the Ga source is turned off. However, significant rate is indicated, as circled in red, due to the increasing background pressure. The false rate is nearly equal in magnitude to the desired Ga rate, resulting, no doubt, in a significant deviation between the actual and intended Ga rates during the third stage. Ar emits efficiently at a multitude of wavelengths upon electron excitation, and is therefore expected to have a similar effect on the signal.
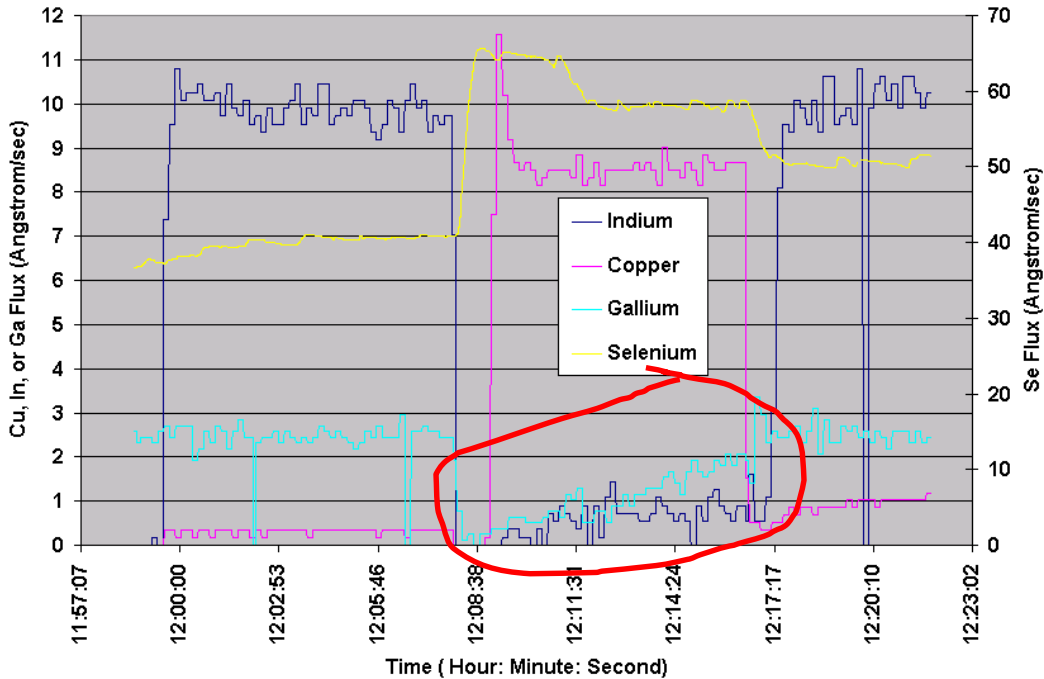
Figure 15: Apparent flux as a function of time for three-stage CIGS deposition, with effect of background pressure increase due to outgassing circled in red.

In order to avoid interference between the EIES and Ar from the PACE sources, an alternate deposition procedure will be implemented. This procedure will involve setting metals source rates using the EIES (without Ar flowing to the PACE source), holding the metals sources at constant deposition power while the PACE source is operating, and judging the end of the second and third stages utilizing the film emissivity. This procedure is similar to that described by Kessler et al[8] to maintain accurate control of maximum and final Cu ratio without the use of a multi-species rate monitor. The new procedure must be flexible enough to allow for some variation in background Ar pressures due to source-to-source differences in reactor tubes.

6. Source capacity. *Do the PACE sources hold enough chalcogen for a typical deposition?*

The capacity of the 5.5" PACE source is larger than the capacity of the baffled-box sources currently used in the bell jar.

The plan for incorporating the ICP sources into the CIGS chamber, as enumerated in the items above, marks the third milestone for phase II as specified in the statement of work.

6. Team Activities

ITN and CSM participate in team activities. This participation has included facilitation of absorber sub-team activities, analysis and discussion of team data in absorber sub-team transport studies, admittance spectroscopy measurements on the same samples, attendance and presentations at team meetings, and initial investigations in applying the CSM environmental scanning electron microscope (ESEM) to team stability interests.

7. Publications

The following papers were published during Phase 2:

- S. Kosuarju, C.A. Wolden, I. Repins, "Development of Plasma-assisted Processing for Selenization and Sulfurization of Absorber Layers", Materials Research Society Symposium Proceedings, vol. **763**, (2003), pp. 391-396.

- S. Kosuarju, I. Repins, C. A. Wolden, "Development of Plasma-assisted Processing for Selenization and Sulfurization of Absorber Layers", *Proceedings of the 2003 National Center for Photovoltaics Review Meeting*, (2003).

8. Conclusions

Several conclusions can be drawn from this year's work:

- Plasma-activation was proven to be beneficial in reducing reaction temperatures for all binary precursors utilized in CIGSS formation: In_2Se_3, In_2S_3, Cu_xSe_y, and Cu_xS_y.

- A detailed study of improvements to materials utilization is also underway.

- ICP source development was advanced such that Se is delivered reliably into the plasma reactor tube, rates are controlled acceptably, source size is small enough to fit into the CIGS bell jar, transmitted RF is minimized, base pressures with Ar flow to the PACE source are satisfactory, and Se uniformity is adequate.

- A plan for incorporation of the ICP sources into CIGS co-evaporation was formulated based on initial data from source operation. This plan addresses the deposition environment's rigorous requirements on rate control, geometry, uniformity, resistance to heat and deposition product, and compatibility with the existing and complex sensors in the bell jar.

- Several aspects of the baseline CIGS process, which will serve during the next phase as a testbed for integration of PACE into three-stage co-evaporation, were improved. Consistent incorporation of Ga was established via tuning source PID parameters and improved calibration of the EIES reading. Reproducibility was improved by insuring a consistent Cu-rich excursion of the film growth, using an infrared sensor to monitor the film emissivity change. Overall, best efficiencies in the bell jar were improved from just over 10% last year to 12.5% this year.

9. Continuing work

Major milestones for next year's work are 1) integration of PACE sources into CIGS co-evaporation, 2) demonstration of 12% devices utilizing the advantages of PACE, and 3) specification of the effectiveness of PACE for increased control over S/(S+Se) ratio in binary compounds.

Achieving these milestones will require completion of a number of specific tasks suggested in the description of this year's work, as well as new work related to tailoring the S/(Se+S) ratio. These tasks are listed below:

- To form a more complete picture of plasma source uniformity, work is ongoing to obtain more finely-spaced thickness data, as well as to examine rate and controllability as a function of substrate distance from the aperture.

- Resulting predictions of PACE source uniformity at the bell jar substrate will be verified in-situ.

- When source and substrate configuration is fully-specified in the bell jar, rate control will be re-examined. Relevant matters include evaluating rate control at several source-to-substrate distances, shortening warm-up times, and re-optimizing PID parameters for selected geometry.

- ICP sources will be installed in the CIGS baseline process, including addition of feedthroughs and adequate RF shielding.

- In order to avoid interference between the EIES and Ar from the PACE sources, an alternate rate control deposition procedure will be implemented.

- ICP sources will be operated in conjunction with three-stage CIGS co-evaporation. Film and device quality with and without plasma will be examined for a variety of conditions.

- The study of the effect of PACE on chalcogen utilization for binary films will be completed.

- The CSM benchtop source will be used to examine the selenization of Cu-In-Ga films as a function of temperature and plasma source conditions.

- Minor adjustments to maximize baseline efficiency and reproducibility will continue under the next phase.

- Team activities, including assembling a publication regarding absorber sub-team activities, and reporting on the utility of the ESEM for stability investigations, will be completed.

REPORT DOCUMENTATION PAGE

Public reporting burden for this collection of information is estimated to average 1 hour per response, including the time for reviewing instructions, searching existing data sources, gathering and maintaining the data needed, and completing and reviewing the collection of information. Send comments regarding this burden estimate or any other aspect of this collection of information, including suggestions for reducing this burden, to Washington Headquarters Services, Directorate for Information Operations and Reports, 1215 Jefferson Davis Highway, Suite 1204, Arlington, VA 22202-4302, and to the Office of Management and Budget, Paperwork Reduction Project (0704-0188), Washington, DC 20503.

1. AGENCY USE ONLY (Leave blank)	2. REPORT DATE January 2004	3. REPORT TYPE AND DATES COVERED Phase II Annual Report December 2002–December 2003

4. TITLE AND SUBTITLE
Plasma-Assisted Coevaporation of S and Se for Wide Band Gap Chalcopyrite Photovoltaics: Phase II Annual Report, December 2002–December 2003

5. FUNDING NUMBERS
PVP45001
NDJ-2-30630-11

6. AUTHOR(S)
I. Repins and C. Wolden

7. PERFORMING ORGANIZATION NAME(S) AND ADDRESS(ES)
ITN Energy Systems, Inc., 8130 Shaffer Parkway, Littleton, Colorado 80127
Colorado School of Mines, Golden, Colorado 80401

8. PERFORMING ORGANIZATION REPORT NUMBER

9. SPONSORING/MONITORING AGENCY NAME(S) AND ADDRESS(ES)
National Renewable Energy Laboratory
1617 Cole Blvd.
Golden, CO 80401-3393

10. SPONSORING/MONITORING AGENCY REPORT NUMBER
NREL/SR-520-35515

11. SUPPLEMENTARY NOTES
NREL Technical Monitor: H. Ullal

12a. DISTRIBUTION/AVAILABILITY STATEMENT
National Technical Information Service
U.S. Department of Commerce
5285 Port Royal Road
Springfield, VA 22161

12b. DISTRIBUTION CODE

13. ABSTRACT *(Maximum 200 words):* In this work, ITN Energy Systems (ITN) and lower-tier subcontractor Colorado School of Mines (CSM) explore the replacement of the molecular chalcogen precursors during deposition (e.g., Se_2 or H_2Se) with more reactive chalcogen monomers or radicals (e.g., Se). Molecular species are converted to atomic species in a low-pressure inductively coupled plasma (ICP). Tasks of the proposed program center on development and validation of monatomic chalcogen chemistry, tuning of low-pressure monomer chalcogen sources, and evaluation of plasma-assisted co-evaporation (PACE) for CIGS co-evaporation. Likely advantages of deposition by plasma-enhanced co-evaporation include: (1) Providing potential for lower deposition temperature and/or for better film quality at higher deposition temperature. (2) Providing potential for decreased deposition times. (3) Providing high material utilization efficiency (~90%) that results in less deposition on other parts of the reactor, leading to lower clean up and maintenance costs, as well as longer equipment lifetime. High material utilization efficiency also reduces the total operating pressure, which is beneficial for the design and control of metal co-evaporation. Advantages include minimal metal-vapor beam spread and lower source operating temperatures. (4) Enabling deposition of wide-bandgap copper indium gallium disulfur-selenide (CIGSS) films with controlled stoichiometry. University researchers at CSM are developing and testing the fundamental chemistry and engineering principles. Industrial researchers at ITN are adapting PACE technology to CIGSS co-evaporation and validating PACE process for fabrication of thin-film photovoltaics. In_2Se_3 films, which are used as precursor layers in high-efficiency CIGS depositions, were used this year as the first test case for examining the advantages of PACE listed above. Gradually, the investigation is being extended to the complete high-efficiency three-stage co-evaporation process.

14. SUBJECT TERMS: PV; molecular chalcogen precursors; inductively coupled plasma (ICP); plasma-assisted co-evaporation (PACE); metal-vapor beam; wide-bandgap; copper indium gallium disulfur-selenide (CIGSS); stoichiometry; three-stage co-evaporation process

15. NUMBER OF PAGES

16. PRICE CODE

17. SECURITY CLASSIFICATION OF REPORT Unclassified	18. SECURITY CLASSIFICATION OF THIS PAGE Unclassified	19. SECURITY CLASSIFICATION OF ABSTRACT Unclassified	20. LIMITATION OF ABSTRACT UL